

Supplementary information

A lightweight and low-cost electrode for lithium-ion batteries derived from paper towel supported MOF arrays

Experimental section

Materials synthesis

Synthesis of the Cu-doped Co-ZIF NPAs@PT: The typical synthesis procedure was carried out as follows. First, $\text{Co}(\text{NO}_3)_2 \cdot 6\text{H}_2\text{O}$ (1.33 mmol) and $\text{Cu}(\text{NO}_3)_2 \cdot 3\text{H}_2\text{O}$ (0.67 mmol) were added into 40 mL of deionized (DI) water under ultrasonication treatment. Second, 16 mmol of 2-methylimidazole (2-MIM) was added into 40 mL DI water to form a clear solution. Then, the two solutions were mixed under the intense stirring to obtain a uniform solution. And next, a piece of commercial PT was immersed into the resultant solution. After reaction for 2 hours at room temperature, the Cu-doped Co-ZIF NPAs@PT was rinsed by DI water and ethanol several times and then dried at 70 °C overnight.

Synthesis of the Co-ZIF NPAs@PT and Cu-doped Co-ZIF NPAs@CC: For comparison, the Co-ZIF NPAs@PT and Cu-doped Co-ZIF NPAs@CC samples were also prepared by the same method as the Cu-doped Co-ZIF NPAs@PT. The Co-ZIF NPAs@PT was synthesized using 2 mmol of $\text{Co}(\text{NO}_3)_2 \cdot 6\text{H}_2\text{O}$ without the dosage of $\text{Cu}(\text{NO}_3)_2 \cdot 3\text{H}_2\text{O}$. And the Cu-doped Co-ZIF NPAs@CC was prepared by replacing carbon cloth (CC) with PT.

Synthesis of the Cu-doped Co/CoO/NC NPAs@CP, Co/CoO/NC NPAs@CP and Cu-doped Co/CoO/NC NPAs@CC: The as-synthesized Cu-doped Co-ZIF NPAs@PT, Co-ZIF NPAs@PT and Cu-doped Co-ZIF NPAs@CC were annealed under Ar/H₂ atmosphere at 500 °C for 2 hours at a ramping rate of 2 °C min⁻¹.

Materials characterization

The phase purity and composition of the samples were characterized by a X-ray diffractometer (XRD, D/maxUltimaIII, Rigaku, Japan). The morphological observations of the as-synthesized products were investigated using field emission scanning electron microscope (FESEM, Supra55, Zeiss, Germany) with an energy dispersive X-ray spectrometer (EDX) and transmission electron microscope (TEM, Tecnai G2 F20 S-TWIN). The X-ray photoelectron spectroscopy (XPS, Thermo Fisher Scientific, ESCALAB 250) measurements were further conducted

out to analyzed the chemical composition and the valence states of the samples. The specific surface area and pore size distribution of the Cu-doped Co/CoO/NC NPAs@CP and Cu-doped Co/CoO/NC NPAs@CC were calculated based on nitrogen adsorption/desorption isotherms (Micromeritics ASAP 2020).

Electrochemical measurements

The as-synthesized products were directly evaluated as binder-free anode electrodes. Celgard 2400 membrane was used as the separator and the electrolyte was 1 M LiPF₆ in ethylene carbonate (EC)/dimethyl carbonate (DMC)/diethyl carbonate (DEC) (1:1:1 by volume). The CR2025 coin-type cells were fabricated in an argon-filled glovebox with the O₂ and H₂O concentrations lower than 0.5 ppm. Discharge/charge experiments of the samples were carried out galvanostatically in the voltage range of 0.01-3.00 V (vs. Li⁺/Li) by using a CT2001A LAND battery test system. The cyclic voltammetry (CV) tests and electrochemical impedance spectroscopy (EIS) measurements were carried out at by using electrochemical workstation (CHI660E). The specific capacities of the electrodes were calculated based on the weight of total electrodes.

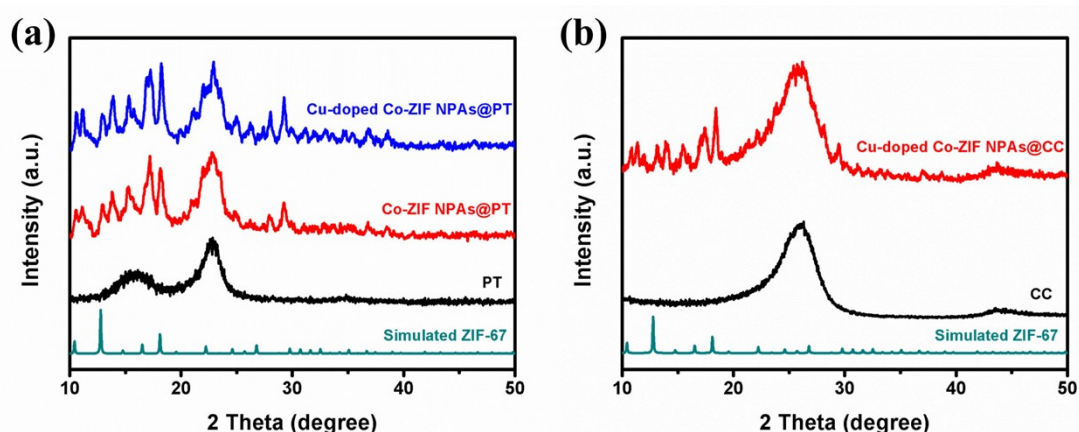


Fig. S1. XRD patterns of (a) the Cu-doped Co-ZIF NPAs@PT, Co-ZIF NPAs@PT and (b) Cu-doped Co-ZIF NPAs@CC.

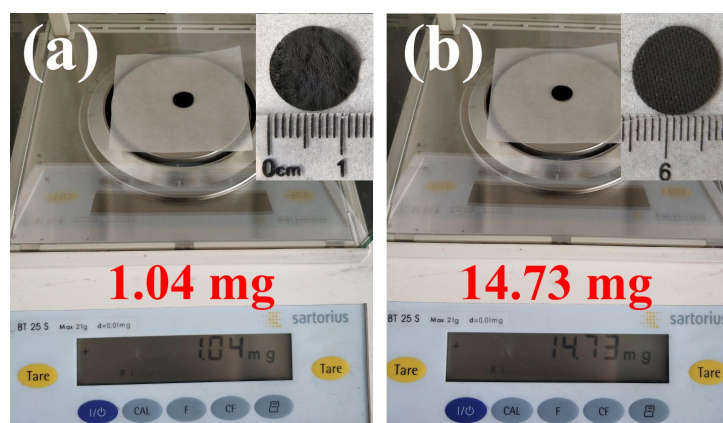


Fig. S2. The weight comparison of (a) Co/CoO/NC NPAs@CP and (b) Cu-doped Co/CoO/NC NPAs@CC electrodes.

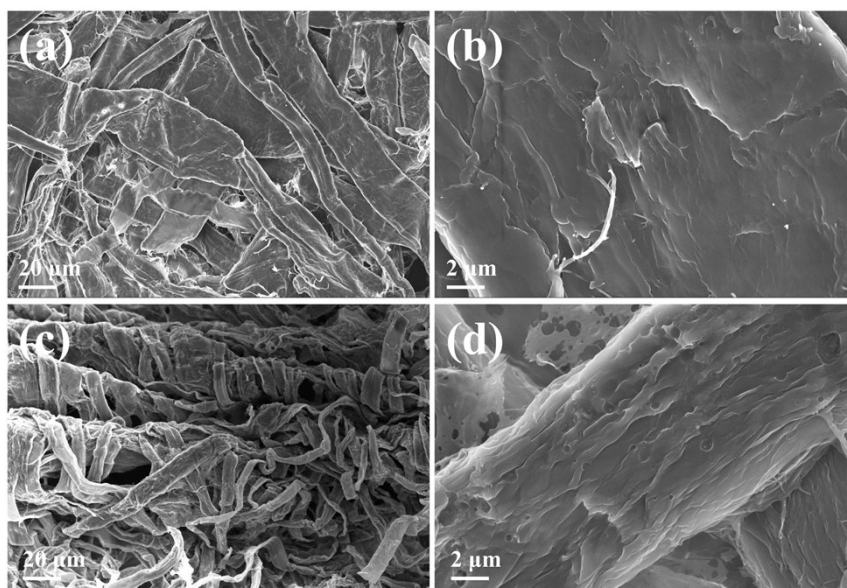


Fig. S3. SEM images of the (a, b) PT and (c, d) CP substrate.

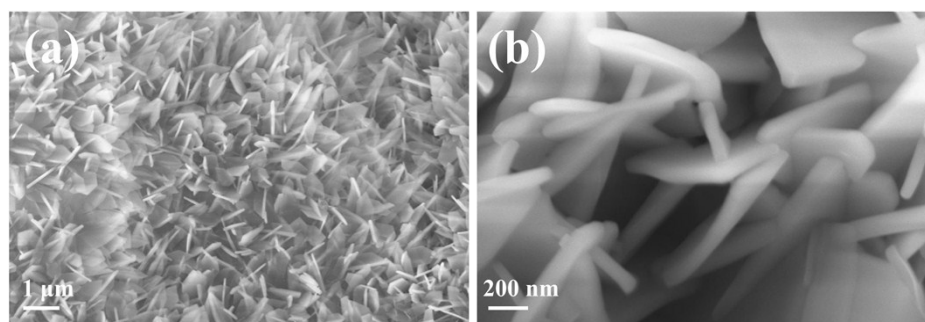


Fig. S4. SEM images of the Co-ZIF NPAs@PT.

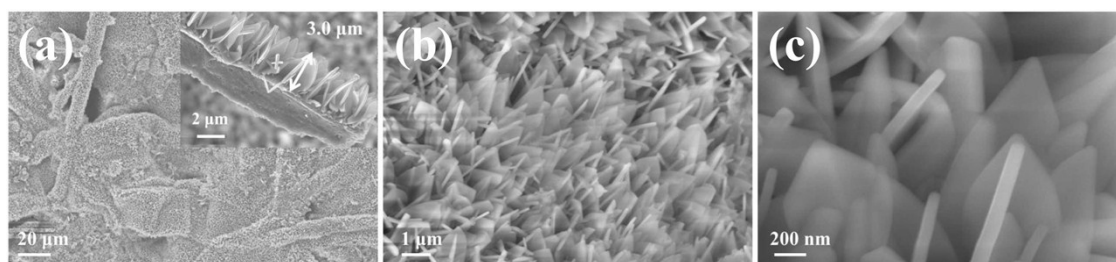


Fig. S5. SEM images of the Cu-doped Co-ZIF NPAs@PT.

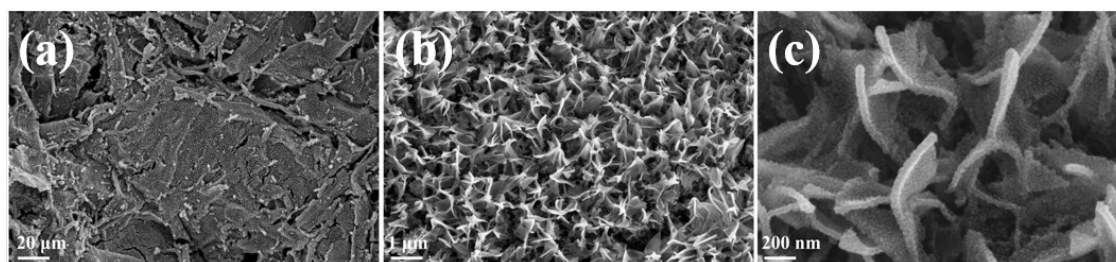


Fig. S6. SEM images of the Co/CoO/NC NPAs@CP.

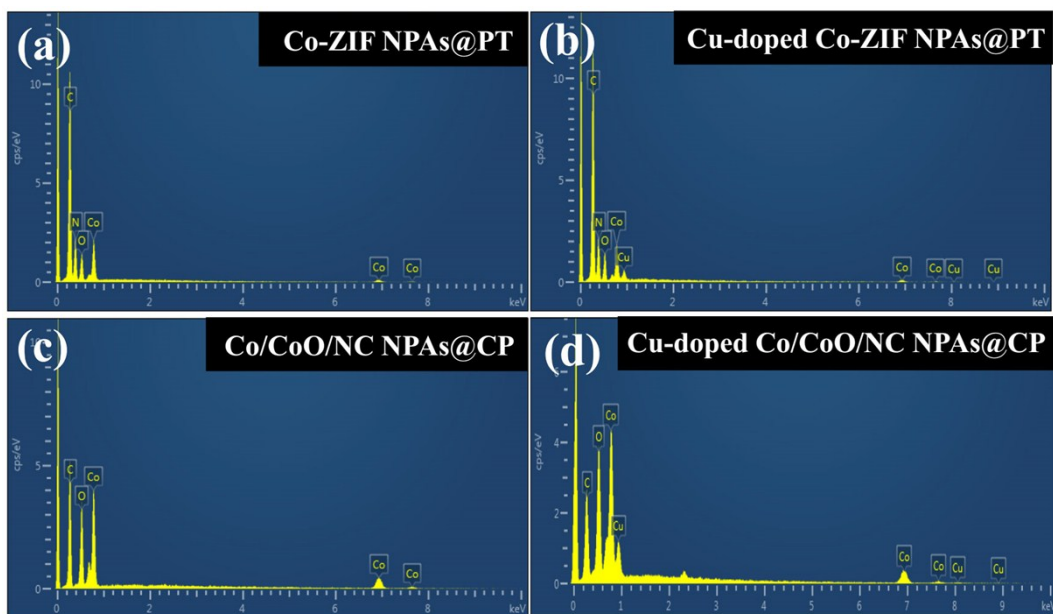


Fig. S7. EDX spectra of the (a) Co-ZIF NPs@PT, (b) Cu-doped Co-ZIF NPs@PT, (c) Co/CoO/NC NPs@CP and (d) Cu-doped Co/CoO/NC NPs@CP.

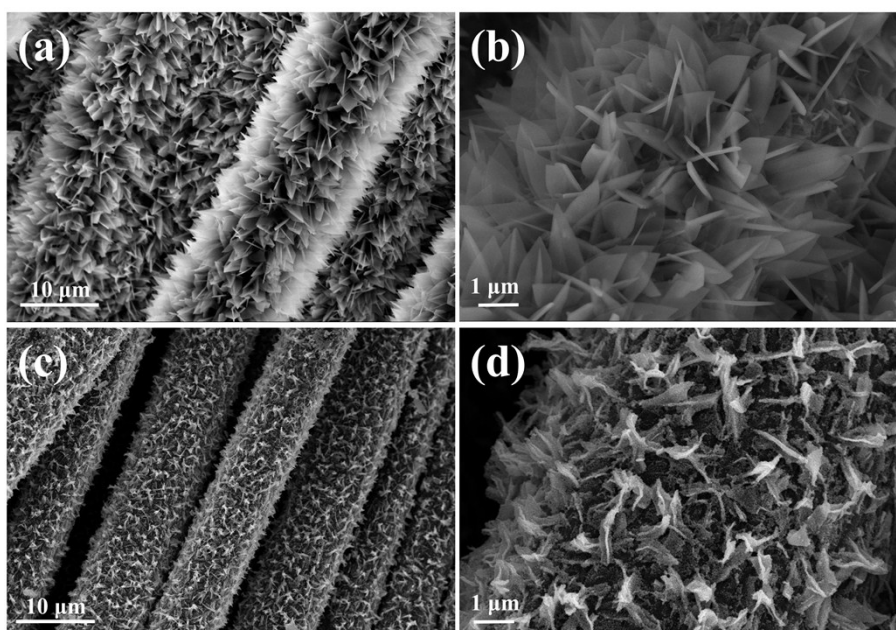


Fig. S8. SEM images of the (a, b) Cu-doped Co-ZIF NPs@CC and (c, d) Cu-doped Co/CoO/NC NPs@CC.

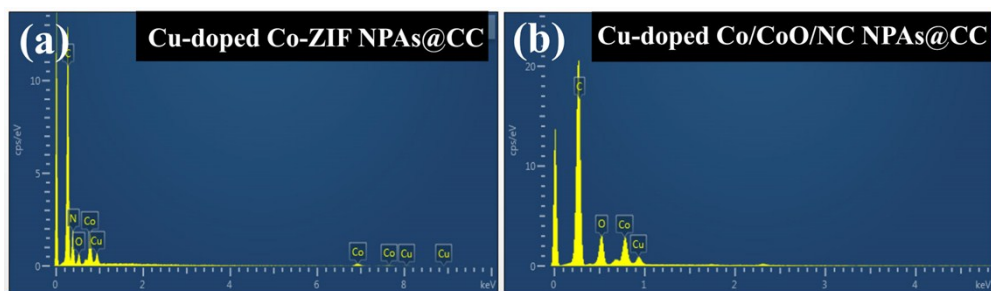


Fig. S9. EDX spectra of the (a) Cu-doped Co-ZIF NPAs@CC and (b) Cu-doped Co/CoO/NC NPAs@CC.

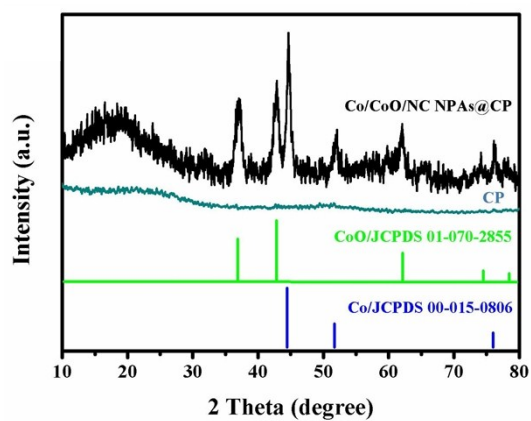


Fig. S10. XRD pattern of the Co/CoO/NC NPAs@CP.

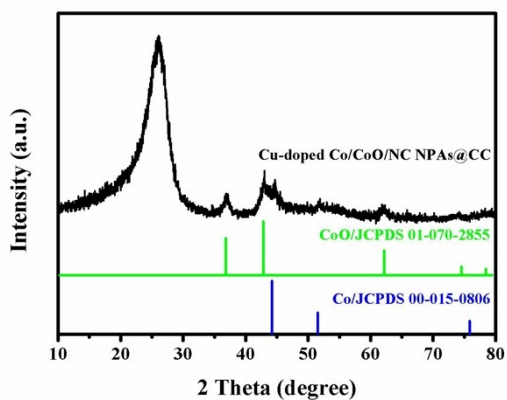


Fig. S11. XRD pattern of the Cu-doped Co/CoO/NC NPAs@CC.

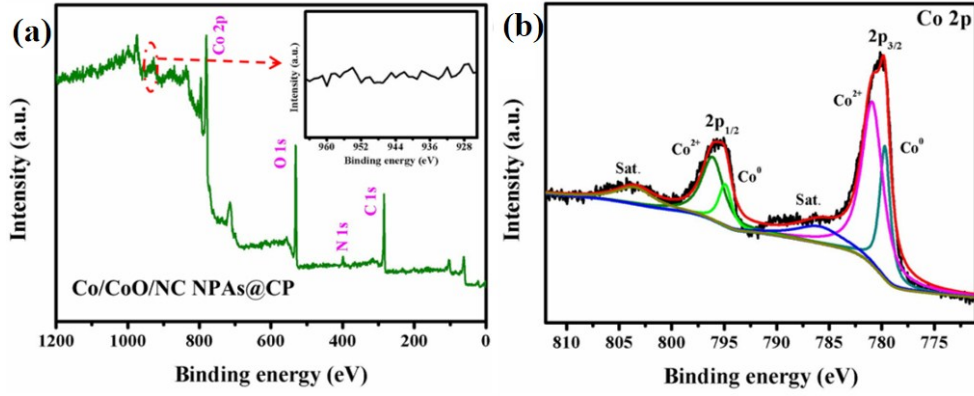


Fig. S12. (a) XPS survey spectrum and (b) high-resolution Co 2p spectrum of the Co/CoO/NC NPAs@CP.

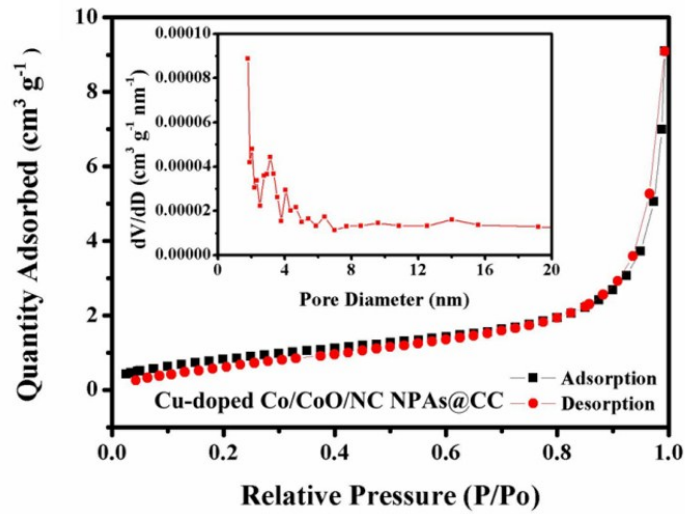


Fig. S13. N₂ adsorption-desorption isotherms and their pore size distribution of the Cu-doped Co/CoO/NC NPAs@CC.

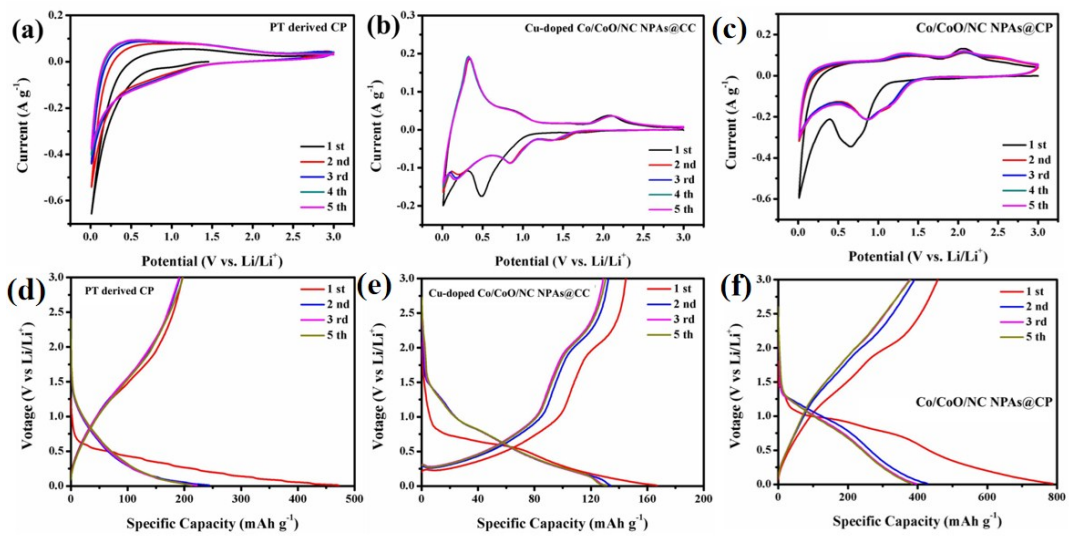


Fig. S14. CV and GCD curves of (a, d) CP, (b, e) Cu-doped Co/CoO/NC NPAs@CC and (c, f) Co/CoO/NC NPAs@CP

at 100 mA g⁻¹.

Table S1. Comparison of the Initial coulombic efficiency with previously reported carbon-based materials.

Materials	Current density (mA g^{-1})	Initial coulombic efficiency	Ref.
Cu-doped Co/CoO/NC NPAs@CP	100	63.6%	This work
ZnO-C yolk-shell microspheres	100	55.7%	1
Nitrogen-doped porous carbon	100	58.4%	2
MnO@C composite	100	54.9 %	3
MoO ₂ @C composite	100	54.8%	4
CuO nanorod arrays	100	56.0%	5
NiSb-embedded carbon hollow spheres	100	53.8%	6
Porous ZnO/C nanocages	100	52.9%	7
Fe ₃ O ₄ /carbon microspheres	100	56.2%	8
ZnO quantum dot/carbon composite	25	55.0%	9

Table S2. Comparison of the performance with previously reported TMOs-based anode materials.

Materials	Current density/ mA g^{-1}	Cycle number	Reversible capacities/ mA h g^{-1}	Rate capacity/ mA h g^{-1} (mA g^{-1})	Ref.
Cu-doped Co/CoO/NC NPAs@CP	100	100	521.2	305.4(1000)	This work
CoO/carbon nanofiber networks	100	52	633	280(2000)	10
Flexible CoO/graphene/carbon nanofiber	500	252	760	400(2000)	11
CoO/graphene	100	150	640	385(6000)	12
CuFe ₂ O ₄ nanofibers	50	50	572.4	354(1000)	13
ZnFe ₂ O ₄ nanofibers	60	30	733	400(800)	14
MnO/CNFs	100	100	1082	~230(1000)	15
CoMoO ₄ @G NFs	100	200	735	360(1000)	16

α -Fe ₂ O ₃ /CNFs	50	75	488	288(500)	17
--	----	----	-----	----------	----

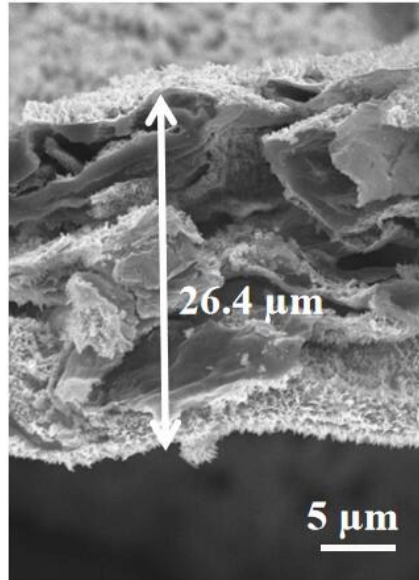


Fig. S15. Cross-section SEM image of the Cu-doped Co/CoO/NC NPAs@CP electrode.

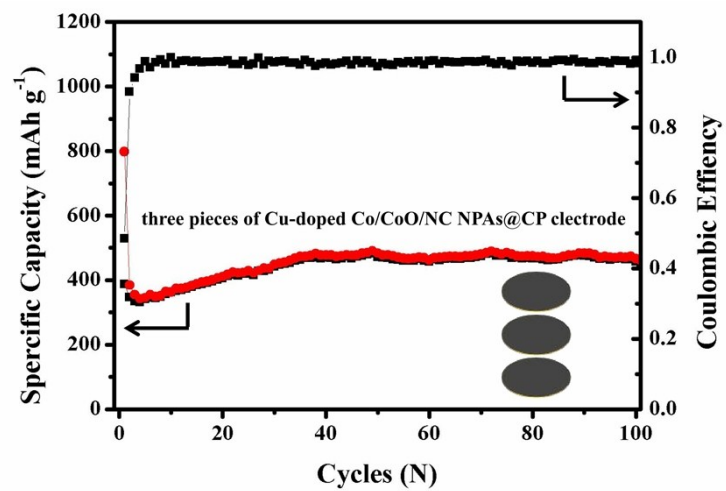


Fig. S16. Cycling stability at 100 mA g⁻¹ of the half cell fabricated by stacking of three pieces of such Cu-doped Co/CoO/NC NPAs@CP electrodes.

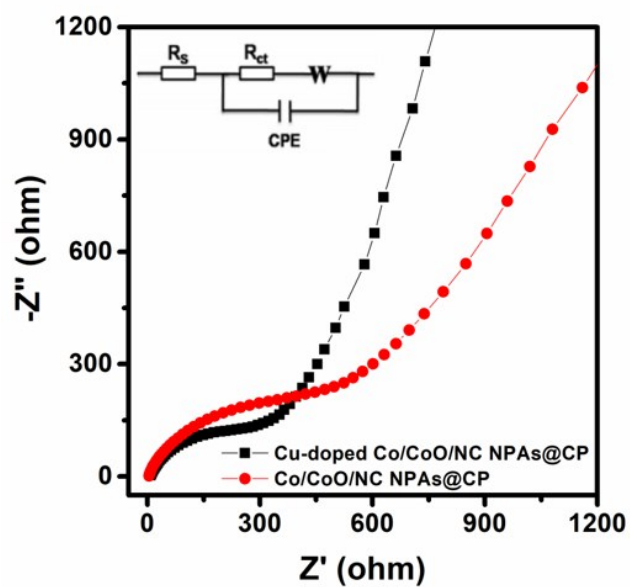


Fig. S17. Nyquist plots of the Cu-doped Co/CoO/NC NPAs@CP and Co/CoO/NC NPAs@CP electrodes.

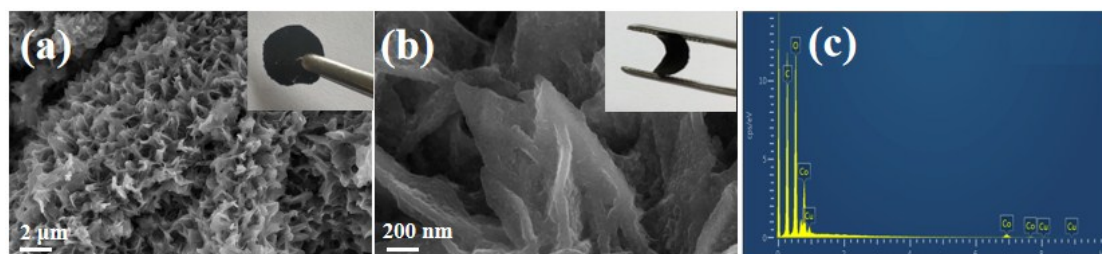


Fig. S18. SEM images and EDX spectrum of the Cu-doped Co/CoO/NC NPAs@CP electrode after 100 cycles (inset the digital photos).

References

- 1 Q. Xie, X. Zhang, X. Wu, H. Wu, X. Liu, G. Yue, Y. Yang and D.-L. Peng, *Electrochim. Acta*, 2014, **125**, 659.
- 2 F. Zheng, Y. Yang and Q. Chen, *Nat. Commun.*, 2014, **5**, 1.
- 3 F. Zheng, G. Xia, Y. Yang and Q. Chen, *Nanoscale*, 2015, **7**, 9637.
- 4 G. Xia, D. Liu, F. Zheng, Y. Yang, J. Su and Q. Chen, *J. Mater. Chem. A*, 2016, **4**, 12434.

- 5 D. Yin, G. Huang, Z. Na, X. Wang, Q. Li, and L. Wang, *ACS Energy Lett.*, 2017, **2**, 1564.
- 6 L. Yu, J. Liu, X. Xu, L. Zhang, R. Hu, J. Liu, L. Yang and M. Zhu, *ACS Appl. Mater. Interfaces*, 2017, **9**, 2516.
- 7 Y. Song, Y. Chen, J. Wu, Y. Fu, R. Zhou, S. Chen and L. Wang, *J. Alloy. Compd.*, 2017, **694**, 1246.
- 8 W. Han, X. Qin, J. Wu, Q. Li, M. Liu, Y. Xia, H. Du, B. Li and F. Kang, *Nano Res.*, 2018, **11**, 892.
- 9 J. F. S. Fernando, C. Zhang, K. L. Firestein, J. Y. Nerkar and D. V. Golberg, *J. Mater. Chem. A*, 2019, **7**, 8460.
- 10 M. Zhang, E. Uchaker, S. Hu, Q. Zhang, T. Wang, G. Cao and J. Li, *Nanoscale*, 2013, **5**, 12342–12349.
- 11 M. Zhang, F. Yan, X. Tang, Q. Li, T. Wang and G. Cao, *J. Mater. Chem. A*, 2014, **2**, 5890–5897.
- 12 X. Huang, R. Wang, D. Xu, Z. Wang, H. Wang, J. Xu, Z. Wu, Q. Liu, Y. Zhang and X. Zhang, *Adv. Funct. Mater.*, 2013, **23**, 4345–4353.
- 13 L. Luo, R. Cui, H. Qiao, K. Chen, Y. Fei, D. Li, Z. Pang, K. Liu and Q. Wei, *Electrochim. Acta*, 2014, **144**, 85–91.
- 14 P. F. Teh, Y. Sharma, S. S. Pramana and M. Srinivasan, *J. Mater. Chem.*, 2011, **21**, 14999–15008.
- 15 B. Liu, X. Hu, H. Xu, W. Luo, Y. Sun and Y. Huang, *Sci. Rep.*, 2014, **4**, 4229.
- 16 J. Xua, S. Gu, L. Fan, P. Xu and B. Lu, *Electrochim. Acta*, 2016, **196**, 125–130.
- 17 L. Ji, O. Toprakci, M. Alcoutlabi, Y. Yao, Y. Li, S. Zhang, B. Guo, Z. Lin and X. Zhang, *ACS Appl. Mater. Interfaces*, 2012, **4**, 2672–2679.